Influence of Creep on Optical Properties of Polypropylene Fibers

K. A. EL-FARAHATY

Physics Department, Faculty of Science, Mansoura University, Mansoura, Egypt

Received 30 January 1997; accepted 2 June 1997

ABSTRACT: The change in some optical properties with the creep extension is measured for polypropylene fibers at several constant applied loads. Multiple-beam Fizeau fringes in transmission are used to determine the mean refractive indices and the mean birefringence of these fibers at different values of creep extensions. Also, the effect of creep extension on the birefringence profile of the fiber is studied. The creep-extension dependence of these optical properties for polypropylene fibers is demonstrated using a stress–strain device connected to a wedge interferometer where the fiber is subjected to a constant load. The results show that under constant load the fiber will extend with time at a rate which decreases as time increases. An empirical formula is suggested to represent the variation of creep extension (%) of polypropylene fibers with time in the time interval of 0–55 min and the constants of this formula are determined. Microinterferograms are given for illustration. © 1998 John Wiley & Sons, Inc. J Appl Polym Sci **67:** 621–627, 1998

INTRODUCTION

Synthetic fibers in the drawn or extended state show considerable optical and mechanical anisotropy. The degree of anisotropy in the drawn state is related to the amount of extension imposed.[1] The relation between the molecular structure of an uniaxially oriented polymer and its optical anisotropy was developed theoretically by Kuhn and Grun.[2] De Vries[3] gave an analysis between the birefringence and the draw ratio of some synthetic fibers. Ward[4] derived expressions for the optical birefringence and elastic moduli of an idealized semicrystalline polymer in terms of the molecular orientation. Pinnock and Ward[5] measured the mechanical and optical properties for a series of poly(ethylene terephthalate) fibers with different draw ratios. Hamza et al.[6–13] studied interferomtrically the optical anisotropy in some synthetic fibers as a function of the draw ratio. Recently, El-Farahaty[14] measured the optomechanical variation produced in undrawn polypropylene fibers by different applied stresses at room temperature.

Multiple- and two-beam microinterferometric techniques were applied to determine the refractive indices and birefringence of the fiber (cf. [1]). Hamza et al.[15,16] derived mathematical expressions for the shape of two-beam interference fringes crossing cylindrical multilayer fibers to determine the refractive indices across the diameter of the fibers (refractive index profile). The effect of the draw ratio[12,13] and the applied stress[14] on the refractive index profile of the fibers was studied interferometrically.

It is now well established that the orientation of crystals caused by stretching a crystalline polymer is time-dependent.[17] The present work reports a study on the influence of creep on some optical properties of polypropylene fibers when they are subjected to a constant load. Investigations were carried out using a multiple-beam microinterferometric technique with a stress–strain device connected to a wedge interferometer.[14]

Journal of Applied Polymer Science, Vol. 67, 621–627 (1998)
 CCC 0021-8995/98/030621-07

EXPERIMENTAL

The sample used in this experiment is of undrawn polypropylene fibers (draw ratio = 1). Multiple-beam Fizeau fringes in transmission were used for the determination of the mean refractive indices, the mean birefringence, and the birefringence profiles for the fibers at different values of creep extensions.

The mean refractive indices $n^{\parallel}$ and $n^{\perp}$ of the fiber for monochromatic light, of wavelength λ, vibrating parallel and perpendicular to the fiber axis, respectively, are given by the following expressions[18]:

$$n^{\parallel} = n_L \pm F^{\parallel}/2A \cdot \lambda/h \tag{1}$$

$$n^{\perp} = n_L \pm F^{\perp}/2A \cdot \lambda/h \tag{2}$$

where n_L is the refractive index of the immersion liquid; $F^{\parallel}$ and $F^{\perp}$ are the areas enclosed by the fringe shift, for light vibrating parallel and perpendicular to the fiber axis, respectively; h is the interfringe spacing corresponding to the wavelength λ, and A is the mean cross-sectional area of the fiber.

The birefringence (Δn) of the fiber can be determined from

$$\Delta n = n^{\parallel} - n^{\perp} \tag{3}$$

The refractive index across the diameter of a cylindrical fiber (index profile) of radius a according to Hamza et al.[16] is given by the following equation:

$$n(r) = \frac{\lambda Z(r)}{2ah(1 - r^2/m^2a^2)^{1/2}} + n_L \frac{(1 - r^2/a^2)^{1/2}}{(1 - r^2/m^2a^2)^{1/2}}$$

$$0 \le r \le a, \quad m > 1 \tag{4}$$

where $n(r)$ is the refractive index of the fiber at a distance r from its center, $Z(r)$ is the fringe shift measured from the interferogram at a distance r' which is calculated from the following equation:

$$r' = a \sin[2 \sin^{-1}(r/ma) - \sin^{-1}(r/a)] \tag{5}$$

and m is given by

$$m = \frac{Z_0\lambda + 2ahn_L}{2ahn_L} \tag{6}$$

where Z_0 is the interference fringe shift inside the fiber at its center and h is the interfringe spacing.

For the case of multiple-beam Fizeau fringes where the fringe displacement is proportional to twice the phase difference introduced by the fiber, the interfringe spacing in eq. (4) must be multiplied by a factor of 2 as follows:

$$n(r) = \frac{\lambda Z(r)}{4ah(1 - r^2/m^2a^2)^{1/2}} + n_L \frac{(1 - r^2/a^2)^{1/2}}{(1 - r^2/m^2a^2)^{1/2}}$$

$$0 \le r \le a, \quad m > 1 \tag{7}$$

Equation (7) gives the relation between the refractive index $n(r)$ across the diameter of the fiber (refractive index profile) and the fringe shift $Z(r)$ for the case of multiple-beam Fizeau fringes. The refractive index profile given by eq. (7) can be calculated for both cases of light vibrating parallel ($n^{\parallel}$) and perpendicular ($n^{\perp}$) to the fiber axis, from which the birefringence profile is calculated according to eq. (3).

Three samples from undrawn polypropylene fibers, each of initial length 7 cm and initial cross-sectional areas of 87.01, 91.43, and 95.95 $\times 10^2$ $(\mu m)^2$, respectively, were investigated under a constant applied load, M = 10, 12, and 15 g, respectively. The extension time range for each sample was 0–55 min at room temperature. The applied mass is reduced to its half-value before taking each interferogram. This was done to overcome the problem of fiber recovery during the exposure time, which was 5 min for each interferogram.

Figures 1(a)–(d) and 2(a)–(d) are microinterferograms showing multiple-beam Fizeau fringes in transmission for light vibrating parallel and perpendicular to the axis of one sample of polypropylene fibers, respectively, at a constant applied load of 10 g. The creep extension for the interferograms [(a)–(d)] is 0, 43, 142, and 228.6%, respectively. Monochromatic light of wavelength λ = 546.1 nm was used, and the refractive index of the immersion liquid was 1.5025 at 18°C.

The fringe shifts in the microinterferograms

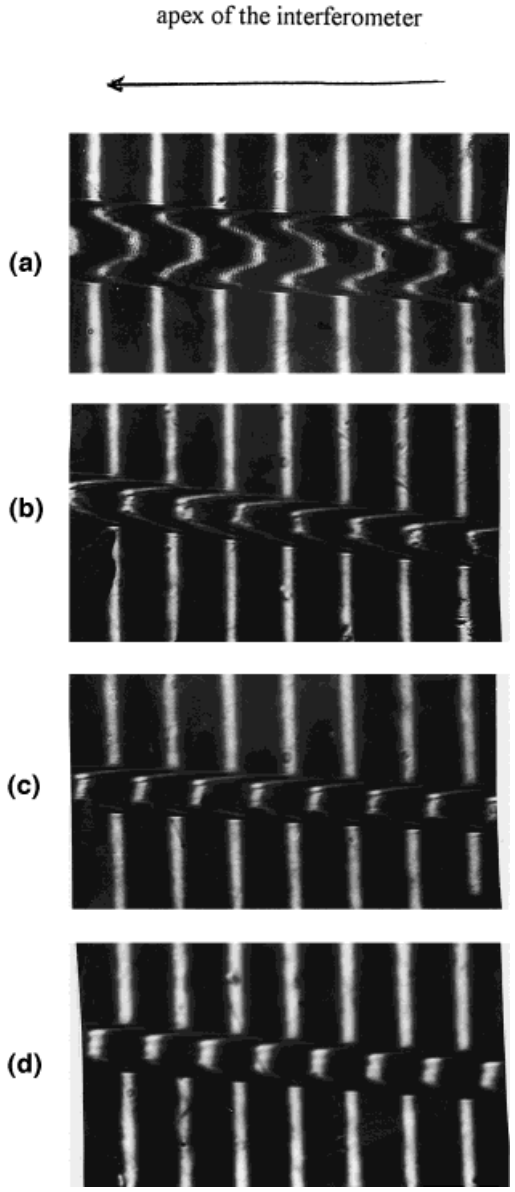

Figure 1 (a–d) Interferograms show multiple-beam Fizeau fringes in transmission for light vibrating parallel to the polypropylene fiber axis at a constant applied load of 10 g and creep extensions of 0, 43, 142, and 228.6%, respectively.

clearly identify differences in optical path variations due to increasing creep extension. Also, it is obvious that, upon extension, the thickness and, hence, the cross-sectional area of the fiber decrease.

Figure 3 interrelates the variation of the cross-sectional area, A, of the fiber with its creep extension, $\varepsilon(t)\%$. It is noticed that there is an initially rapid decrease of the cross-sectional area with the creep extension and the decreasing is seen to occur more slowly with increasing extension.

The variation of the creep extension, $\varepsilon(t)\%$, with time, $t(\text{min})$, is shown in Figure 4. It is clear that, when the fiber is subjected to a constant load, its extension will be a function of the time; generally, the rate of extension decreases as time increases, but may never actually decrease to zero.[19] Also, it is obvious that for a given time creep extension is affected by the value of the applied load. Creep extension, $\varepsilon(t)$, is found to vary with time, t, according to the suggested empirical relation

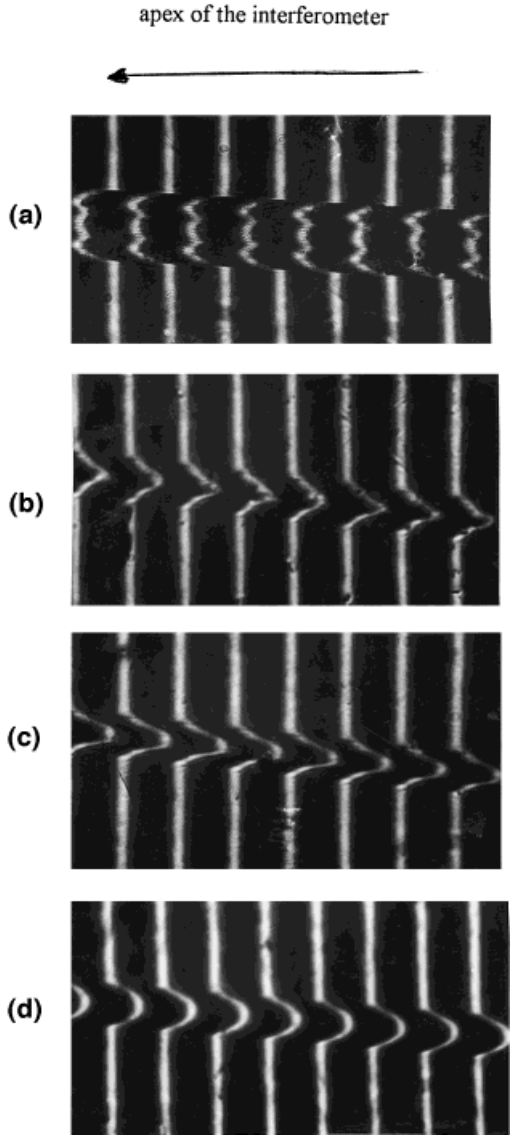

Figure 2 (a–d) Interferograms for the same fiber given in Figure 1 and at the same values of creep extension but for the other direction of light vibrations.

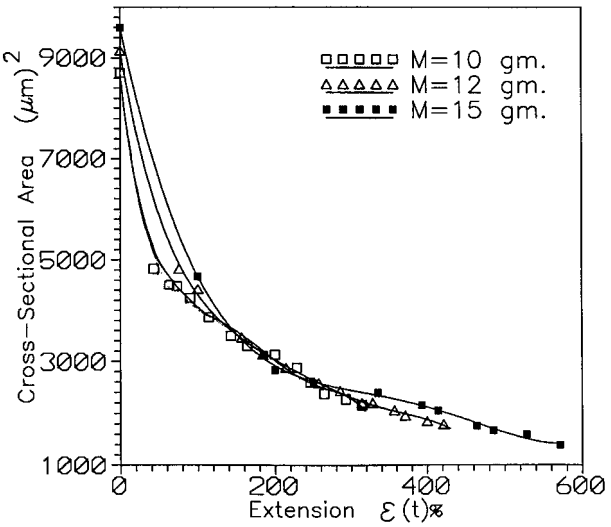

Figure 3 Variation of the cross-sectional area with creep extension (%) at constant applied loads (M = 10, 12, and 15 g).

$$\varepsilon(t) = \varepsilon_0 + p \ln t \qquad (8)$$

where ε_0 and p are functions of applied load for undrawn polypropylene fibers. The values of ε_0 and p for applied loads 10, 12, and 15 g are given in Table I. The good agreement between the experimental values (points) and the theoretical values calculated from eq. (8) (solid line) is illustrated also in Figure 4.

Table I Values of the Constants in Eq. (8) for Undrawn Polypropylene Fibers

Load M (g)	Constant	
	ε_0	p
10	0.704993	72.8614
12	52.008700	91.3231
15	85.694200	114.8610

The mean refractive indices $n^{\parallel}$ and $n^{\perp}$ at each value of creep extension are determined from the fringe shifts as they cross the fiber perpendicular to its axis according to eqs. (1) and (2), respectively. Variation of the mean refractive indices ($n^{\parallel}$, $n^{\perp}$) with the creep extension, $\varepsilon(t)$%, is shown in Figure 5. It is noticed that the influence of creep on polypropylene fibers is to increase the refractive index $n^{\parallel}$ and decrease the refractive index $n^{\perp}$, but the changes in $n^{\parallel}$ are greater and more obvious than those in $n^{\perp}$. This behavior means that during extension the fiber chains become oriented in the direction of extension (parallel to the fiber axis).

The values of the isotropic refractive index (n_{iso}) for polypropylene fibers at different creep extensions are calculated from the experimental values, using the formula $n_{iso} = (n^{\parallel} + 2n^{\perp})/3$. There are small variations in the values of n_{iso}

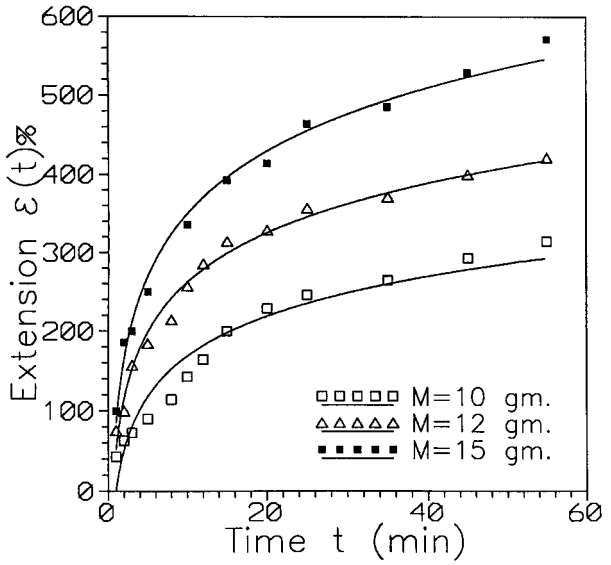

Figure 4 Creep extension (%) as a function of extension time (t, min) at constant applied loads (M = 10, 12, and 15 g).

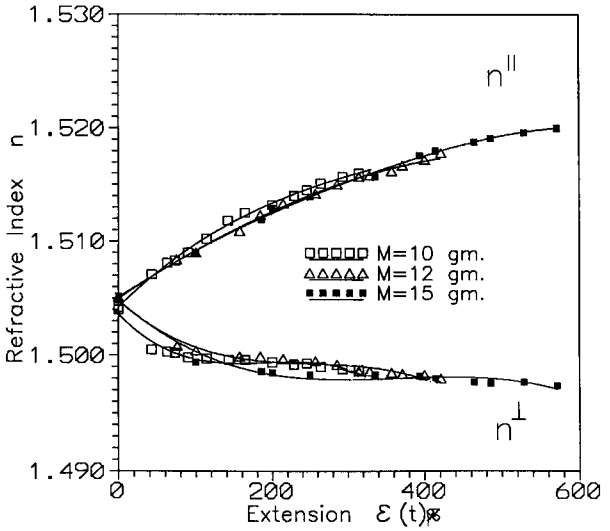

Figure 5 The mean refractive indices ($n^{\parallel}$ and $n^{\perp}$) as a function of creep extension, $\varepsilon(t)$%, at constant applied loads (M = 10, 12, and 15 g).

Table II Values of n_{iso} at Different Creep Extensions, $\varepsilon(t)\%$, for Undrawn Polypropylene Fibers

M = 10 g		M = 12 g		M = 15 g	
$\varepsilon(t)\%$	n_{iso}	$\varepsilon(t)\%$	n_{iso}	$\varepsilon(t)\%$	n_{iso}
43.0	1.5027	75.7	1.5030	100.0	1.5026
62.9	1.5027	100.0	1.5029	186.7	1.5030
72.8	1.5030	157.2	1.5032	200.0	1.5033
90.0	1.5030	185.0	1.5037	255.0	1.5035
142.0	1.5037	257.2	1.5041	335.4	1.5041
200.0	1.5040	314.3	1.5041	392.9	1.5046
228.6	1.5043	328.6	1.5041	414.3	1.5047
243.7	1.5046	357.0	1.5044	464.3	1.5047
264.3	1.5046	371.4	1.5045	485.7	1.5048
292.9	1.5047	400.0	1.5043	528.6	1.5049
314.3	1.5048	421.4	1.5043	579.0	1.5050

with the different creep extensions (Table II), which can be entirely accounted for by the density changes with the corresponding extensions.[20]

The experimental values of the mean birefringence, Δn, are calculated from eq. (3). Figure 6 shows the mean birefringence, Δn, as a function of the creep extension, $\varepsilon(t)\%$. It is clear that there is a steep initial rise in Δn at low values of creep extension, $\varepsilon(t)$, followed by slow increasing at higher values of $\varepsilon(t)$.

The interferograms of multiple-beam Fizeau fringes in transmission for both light vibrating

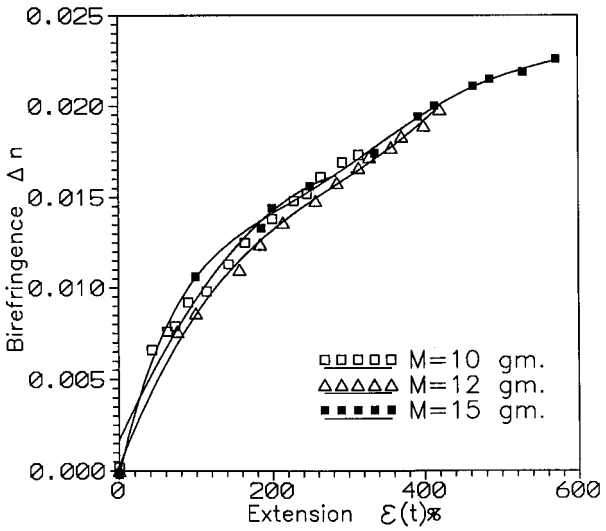

Figure 6 The mean birefringence (Δn) as a function of creep extension, $\varepsilon(t)\%$, at constant applied loads (M = 10, 12, and 15 g).

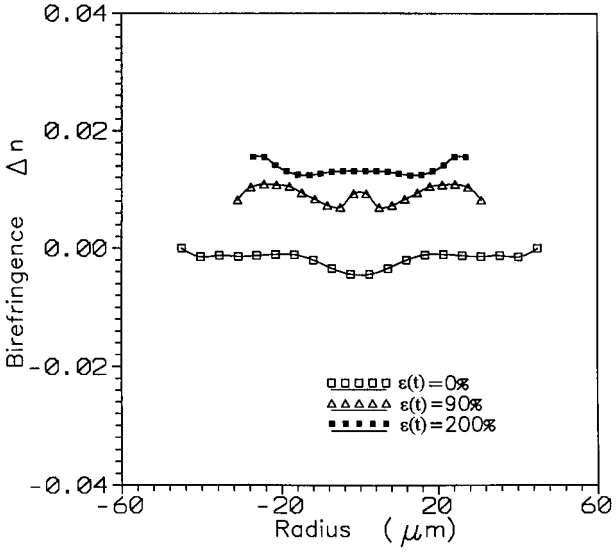

Figure 7 Birefringence profiles of polypropylene fibers with constant applied load (M = 10 g) for creep extension (%) values (0, 90, and 200).

parallel and perpendicular to the polypropylene fiber axis are used to study the variation of the birefringence, Δn, across the diameter of the fiber (birefringence profile) with the aid of eqs. (7) and (3) at different values of creep extension $\varepsilon(t)\%$.

The influence of creep extension on the birefringence profile of polypropylene fibers is illustrated in Figures 7–9, where the fiber is subjected to a

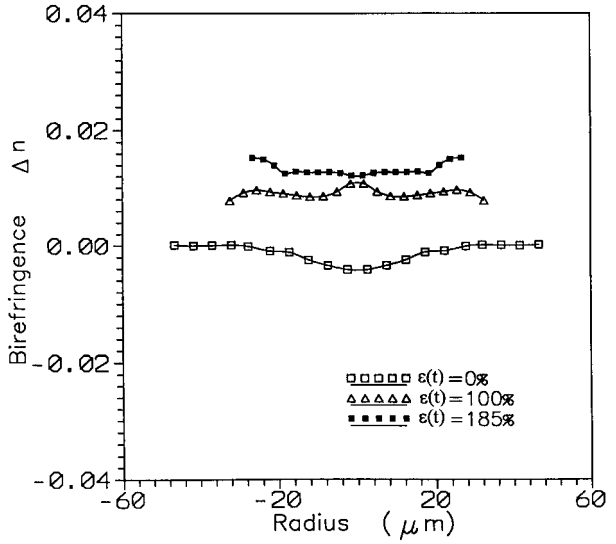

Figure 8 Birefringence profiles of polypropylene fibers with constant applied load (M = 12 g) for creep extension (%) values (0, 100, and 185).

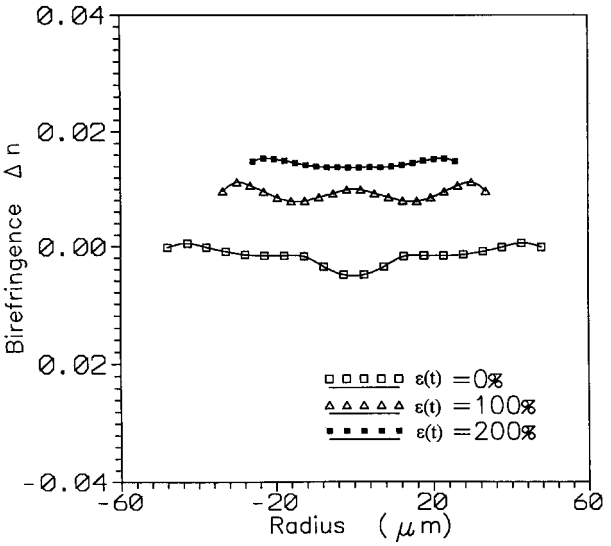

Figure 9 Birefringence profiles of polypropylene fibers with constant applied load (M = 15 g) for creep extension (%) values (0, 100, and 200).

constant load of 10, 12, and 15 g, respectively. The values of creep extension (%) in Figures 7–9 are (0, 90, 200), (0, 100, 185), and (0, 100, 200), respectively.

From the figures of the birefringence profiles, it is noticed that the fiber has a skin–core structure. Also, it is clear that, at equivalent levels of creep extension, the birefringence profile changes in an almost identical behavior for all the given applied loads. This convergency in the birefringence profiles means that creep extension is the main parameter which controls the chain orientation, whatever the value of the constant applied load.

CONCLUSIONS

From the previous investigations, when polypropylene fiber is subjected to a constant load at room temperature, one concludes that

1. The fiber will extend at a rate which decreases as time increases (Fig. 4). The creep extension does not reach an equilibrium value and perceptible changes in strain can be detected even after 1 year.[21] At a given time, the magnitude of $\varepsilon(t)$ increases with increasing the applied load.
2. The suggested formula (8) helps in the testing of mechanical properties of undrawn polypropylene fibers and in monitoring the processing machinery.
3. Upon creep extension, the cross-sectional area of the fiber decreases with a rapid change followed by a region in which the decreasing occurs more slowly.
4. The refractive index of the fiber $n^{\parallel}$ and its birefringence Δn continued to increase with the creep extension $\varepsilon(t)$ (cf. Figs. 5 and 6). This behavior means that the polymer molecules will tend to be aligned parallel to the fiber axis as the fiber is subjected to creep extension and one might relate creep extension to the tensile properties of these fibers.
5. Also, the results of the influence of creep extension on the birefringence profiles show that, at equivalent levels of creep extension (%), the birefringence profiles are converged whatever the magnitude of the constant applied load (cf. Figs. 7–9). This behavior confirms that creep extension is the main parameter which controls chain orientation.

Generally, the above results and considerations emphasize that multiple-beam Fizeau fringes with the aid of a stress–strain device is a very promising technique in the investigation of the optomechanical properties of fibers.

REFERENCES

1. N. Barakat and A. A. Hamza, *Interferometry of Fibrous Materials,* Adam Hilger, Bristol, 1990.
2. W. Kuhn and F. Grun, *Kolloid Z.,* **101,** 248–271 (1942).
3. H. J. De Vries, *Polym. Sci.,* **34,** 761–778 (1959).
4. I. M. Ward, *Proc. Phys. Soc.,* **80,** 1176–1188 (1962).
5. P. R. Pinnock and I. M. Ward, *Br. J. Appl. Phys.,* **15,** 1559–1568 (1964).
6. A. A. Hamza and M. A. Kabeel, *J. Phys. D Appl. Phys.,* **20,** 963–968 (1987).
7. A. A. Hamza, I. M. Fouda, K. A. El-Farahaty, and S. A. Helaly, *Polym. Test.,* **7,** 329–343 (1987).
8. A. A. Hamza, K. A. El-Farahaty, and S. A. Helaly, *Opt. Appl.,* **18,** 133–141 (1988).
9. A. A. Hamza, I. M. Fouda, M. A. Kabeel, and H. M. Shabana, *Polym. Test.,* **8,** 201 (1989).
10. A. A. Hamza, I. M. Fouda, K. A. El-Farahaty, and E. A. Seisa, *Polym. Test.,* **10,** 83–90 (1991).

11. A. A. Hamza, I. M. Fouda, K. A. El-Farahaty, and E. A. Seisa, *Polym. Test.,* **10,** 195–203 (1991).
12. A. A. Hamza, I. M. Fouda, T. Z. N. Sokkar, M. M. Shahin, and E. A. Seisa, *Polym. Test.,* **11,** 233–245 (1992).
13. A. A. Hamza, I. M. Fouda, T. Z. N. Sokkar, M. M. Shahin, and E. A. Seisa, *Polym. Test.,* **11,** 297–307 (1992).
14. K. A. El-Farahaty, *Polym. Test.,* **15,** 163–177 (1996).
15. A. A. Hamza, T. Z. N. Sokkar, and M. M. Shahin, *J. Appl. Phys.,* **70,** 4480–4484 (1991).
16. A. A. Hamza, T. Z. N. Sokkar, and W. A. Ramadan, *Pure Appl. Opt.,* **1,** 321–336 (1992).
17. T. Oda and R. S. Stein, *J. Polym. Sci. Part A-2,* **10,** 685–691 (1972).
18. A. A. Hamza, T. Z. N. Sokkar, and M. A. Kabeel, *J. Phys. D Appl. Phys.,* **18,** 1773–1780 (1985).
19. H. J. Woods, *Physics of Fibres,* The Institute of Physics, London, 1955, Chap. 5.
20. H. Angad Gaur and H. de Vries, *J. Polym. Sci.,* **13,** 835–850 (1975).
21. N. J. Abbott and R. B. Beevers, *Experiments in Fibre Physics,* Butterworths, London, 1970, p. 78.